ELSEVIER

Seminars in
NUCLEAR
MEDICINE

Pediatric Nuclear Medicine in Acute Care

Amer Shammas, MD, Reza Vali, MD, and Martin Charron, MD*

Various radiopharmaceuticals are available for imaging pediatric patients in an acute care setting. This article focuses on the common applications used on a pediatric patient in acute care. To confirm the clinical diagnosis of brain death, brain scintigraphy is considered accurate and has been favorably compared with other methods of detecting the presence or absence of cerebral blood flow. Ventilation-perfusion lung scans are easy and safe to perform with less radiation exposure than computed tomography pulmonary angiography and remain an appropriate procedure to perform on children with suspected pulmonary embolism as a first imaging test in a hemodynamically stable patient with no history of lung disease and normal chest radiograph. ^{99m}Tc pertechnetate scintigraphy (Meckel's scan) is the best noninvasive procedure to establish the diagnosis of ectopic gastric mucosa in Meckel's diverticulum. Hepatobiliary scintigraphy is the most accurate diagnostic imaging modality for acute cholecystitis. ^{99m}Tc-dimercaptosuccinic acid scintigraphy is the simplest, and the most reliable and sensitive method for the early diagnosis of focal or diffuse functional cortical damage. Bone scintigraphy is a sensitive and noninvasive technique for the diagnosis of bone disorders such as osteomyelitis and fracture. Of recent, positron emission tomography imaging using ^{18}F-NaF has been introduced as an alternative to bone scintigraphy. ^{18}F-fluorodeoxyglucose-positron emission tomography has the potential to replace other imaging modalities, such as the evaluation of fever of unknown origin in pediatric patients, with better sensitivity and significantly less radiation exposure than gallium scan.
Semin Nucl Med 43:139-156

Various radiopharmaceuticals are available for imaging pediatric patients in acute care with newly developed imaging techniques such as single photon emission computed tomography (SPECT)/computed tomography (SPECT/CT) and positron emission tomography (PET)/CT. This review describes the most common established examinations in pediatric nuclear medicine in acute care setting.

The article covers brain imaging for brain death, ventilation, and perfusion study and the interpretation for pulmonary embolism (PE) in children, Meckels scan for pediatric lower gastrointestinal (GI) bleeding, renal cortical imaging for pyelonephritis, bone scintigraphy in various skeletal abnormalities including osteomyelitis, fractures, and non-accidental injuries and finally the emerging role of ^{18}F-fluorodeoxyglucose (FDG)-PET in fever of unknown origin in children.

Diagnostic Imaging, Nuclear Medicine Division, The Hospital for Sick Children, University of Toronto, Toronto, ON, Canada.
*Address reprint requests to Martin Charron, MD, Department of Diagnostic Imaging, Division of Nuclear Medicine Hospital for Sick Children, 555 University Avenue, Toronto, ON, Canada M5G 1X8.
E-mail: martin.charron@sickkids.ca

General Consideration

Appropriate communication between an experienced nuclear medicine staff and children or parents is essential to obtain their cooperation. A clear explanation of the study should be given to the parents, as well as children if they are old enough, in simple terms. Allowing a parent to maintain close contact with the child, or having the child watch DVD movies during the study, helps to relax and distract attention away from the procedure and minimizes movement. Immobilization, using a safety belt and gently wrapping a bed sheet if needed, requires well-trained staff and patience and should be judiciously exercised.[1,2] A quiet environment with dim light may help younger children to fall asleep during the test. In addition, motion correction techniques can be used to improve the image quality.[2]

The need for sedation or anesthesia must be assessed individually for children in a situation where good quality imaging cannot be obtained without significant motion. Generally, sedation or anesthesia protocols are somewhat variable and performed in accordance with individual institutional guidelines. Guidelines from the American College of Radiology and the American Academy of Pediatrics or Society

0001-2998/12/$-see front matter
http://dx.doi.org/10.1053/j.semnuclmed.2012.10.001

of Nuclear Medicine (SNM) can help in developing an appropriate institutional sedation protocol.[1]

Generally, pediatric activity doses are calculated using adult dose adjusted for body weight, body surface area, or age. However, there is no universally accepted guideline for pediatric radiopharmaceutical administered doses. Recently, a new North American consensus guideline was published and approved by the SNM addressing the minimum dose for the smallest patients and recommended doses on the basis of body weight for commonly used radiopharmaceuticals in pediatric nuclear medicine.[3] European Association of Nuclear Medicine also introduced a pediatric dosage card for major nuclear medicine diagnostic procedures.[4]

Brain Scintigraphy for Brain Death

Brain death in neonates, infants and children relies on a clinical diagnosis that is based on the absence of neurologic function with a known irreversible cause of coma. Coma and apnea must coexist to diagnose brain death. This diagnosis should be made by physicians who have evaluated the history and completed the neurologic examinations.[5,6] The diagnosis of brain death based on neurologic examination alone should not be made if supratherapeutic or high therapeutic levels of sedative agents have been administered. If uncertainty remains, an additional study such as brain scintigraphy should be performed, although this study is not a substitute for the neurologic examination.

Based on the guidelines for determination of brain death in infants and children from the American Academy of Pediatrics, additional studies can be used to help in making the diagnosis of brain death to reduce the observation period, or when components of the examination or apnea testing cannot be completed safely, or if there is uncertainty about the results of the neurologic examination, or if a medication effect may interfere with evaluation of the patient. If the ancillary study supports the diagnosis, a second examination and apnea testing can then be performed.[5] In some countries other than the United States, a confirmatory test is required by law.[7]

Radiopharmaceuticals and Imaging Technique

Conventional cerebral radionuclide angiography followed by planar scintigraphy with ^{99m}Tc-pertechnetate or ^{99m}Tc-diethylenetriamine pentaacetic acid (DTPA) can be used in children with an equivocal clinical diagnosis of brain death which is based on flow images followed by static planar images in anterior and lateral projections.[8,9] However, imaging with brain-specific tracers such as ^{99m}Tc-ethyl cysteinate dimer (ECD) or ^{99m}Tc-hexamethylpropyleneamine oxime (HMPAO) has currently been used more frequently, allowing superior definition (visualization) of posterior fossa and brain stem perfusion.[10,11] Brain-specific agents are preferred and are the agents of choice, as interpretation is less dependent on the quality of the bolus and early dynamic component. These agents allow the assessment of cerebral flow not only on the first pass flow images but also on regional cerebral tissue perfusion and hence brain viability on delayed planar images. Spieth et al.[12] suggested that ^{99m}Tc-HMPAO is a superior agent for cerebral perfusion studies to determine brain death. Unlike ^{99m}Tc-DTPA, ^{99m}Tc-HMPAO is also able to normally identify the gray matter of the cerebellum, midbrain, and medulla. These areas must be evaluated to ensure that they meet the strict criteria for brain death. The Brain Imaging Council of the SNM feels that although individual laboratories may use nonspecific brain tracers such as ^{99m}Tc-DTPA and ^{99m}Tc-pertechnetate, these are less commonly used than ^{99m}Tc-ECD or ^{99m}Tc-HMPAO for assessment of cerebral perfusion.[8] The typical dose for children is 11.1 MBq/kg (0.3 mCi/kg) with a minimum dose of 185 MBq (5 mCi). Flow images are acquired at the time of tracer injection at 1 s/frame for 60 seconds. If better spatial resolution is required images can be combined into 2 s/frame. If nonspecific agents are used, static planar images are acquired in anterior and lateral views and posterior if possible. If specific brain perfusion tracers are used, planar images should be acquired approximately after 20 minutes in addition to the flow images.[8] SPECT could be performed in addition to flow images providing better visualization. It can be helpful for differentiating overlying scalp from intracranial activity and for evaluating the posterior fossa.[13]

Interpretation

When nonspecific agents are used, the lack of flow in a dynamic flow study on anterior view, in combination with the absence of activity in the venous sinus on static images, confirms the clinical diagnosis of brain death. However, faint activity of venous sinuses may be seen in children with nonspecific brain tracers, which makes it difficult to interpret. Coker and Dillehay[14] reported sinus activity in 14 of 55 children who had brain death.

Using specific agents such as ^{99m}Tc-HMPAO, the planar or SPECT images should demonstrate no cerebral or cerebellar activity in addition to absence of brain flow (Fig. 1)[11]. Usually, this brain imaging study is not affected by drug intoxication or hypothermia as the EEG may be, and is more specific for brain death. The sensitivity of planar imaging using ^{99m}Tc-HMPAO is very high and the specificity is virtually 100%. To evaluate the reliability of SPECT imaging in the diagnosis of brain death, Facoo et al. evaluated 50 comatose patients with SPECT imaging using ^{99m}Tc-HMPAO. All patients tested in pre-terminal conditions showed preserved brain perfusion. SPECT imaging confirmed the diagnosis of brain death in 45 out of 47 patients (95.7%). Activity in the basal ganglia, thalamus or brain stem was noted in 2 clinically brain-dead infants.[15] In infants, brain uptake may be present despite the clinical diagnosis of brain death. Ashwal and Schneider[16] reported a brain uptake in 6 of 17 infants with clinical brain death, 3 of them were preterm infants.The remaining 11 infants had no cerebral blood flow. Okuyaz et al. also reported 2 newborns needed a second image to confirm the diagnosis. In this study, 8 patients who fulfilled the clinical criteria of brain death were evaluated using ^{99m}Tc-HMPAO SPECT and

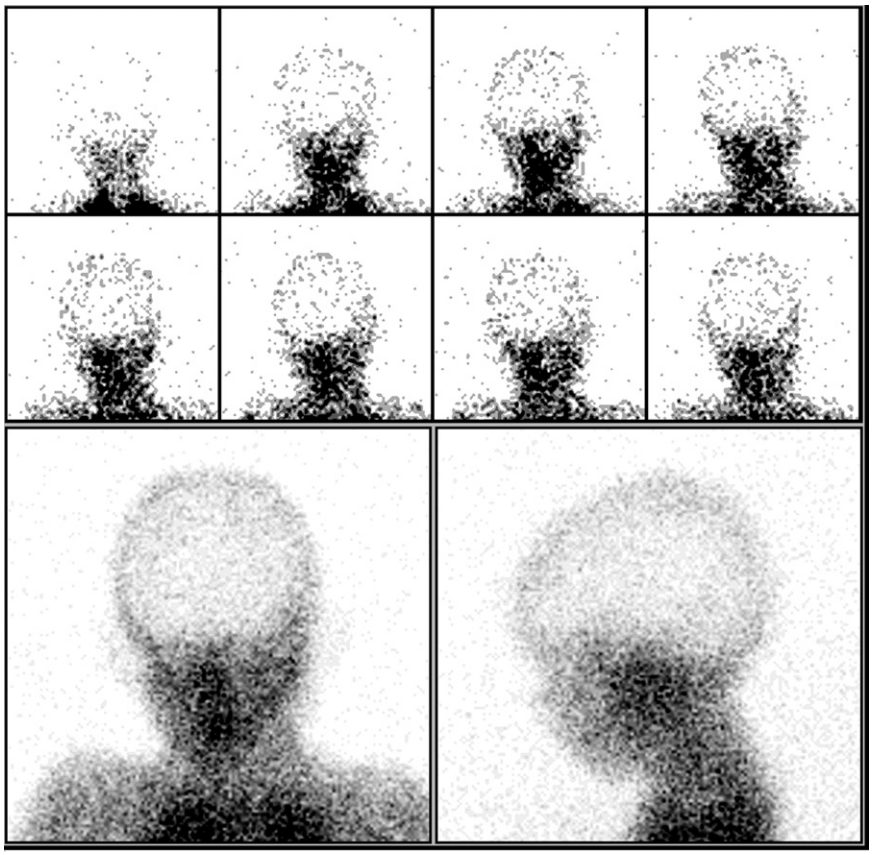

Figure 1 ^{99m}Tc-HMPAO exam for evaluation of brain death in a 4-year old boy. Early flow images as well as delayed anterior and left lateral views did not show any cerebral or cerebellar activity.

6 patients demonstrated lack of perfusion activity in the cerebrum in their first SPECT study.[10]

In summary, brain scintigraphy for brain death in children is accurate and has been favorably compared with other methods of detecting the presence or absence of cerebral blood flow. Brain-specific agents such as ^{99m}Tc-HMPAO are preferred. Flow study followed by planar static images is usually obtained. SPECT imaging can also be performed. Cerebral blood flow may be detected in infants who are clinically brain dead and repeating the study may be required later to demonstrate no perfusion and confirm brain death diagnosis.

V/Q Scans for PE

PE in the pediatric population is relatively less common in children than in adults. However, improvements in pediatric care have led to increased survival of chronic or critically ill children and, thus, increase in the risk and the incidence of common complications encountered by such patients, including PE.[17]

The incidence of PE in children with deep venous thrombosis in a Canadian registry of pediatric patients was 5.3 of 10,000 hospital admissions and 0.07 of 10,000 of the general population of children in Canada. However, only 23% of children were evaluated for PE by ventilation-perfusion lung scan (V/Q scan) (31of 137 children). PE was diagnosed in 22 patients based on high probability scans with an incidence of 0.86 per 10,000 hospital admissions. This incidence is likely underestimated due to low possibility of PE in children, suggesting that in the pediatric population, physicians often do not consider PE in their differential diagnosis and do not perform the testing necessary to make the diagnosis.[17,18] Buck et al. reviewed the autopsies in children and found a PE incidence of 4%. They concluded that PE in children is under diagnosed and using lung perfusion scintigraphy should be encouraged.[19] One of the largest single center-based reports of PE in children published to date reported an incidence of 5.7/10,000 admissions in The Hospital for Sick Children, Toronto, significantly higher than previously reported for Canadian pediatric PE.[20]

Cancer, immobility, central venous lines, vascular malformations, nephrotic syndrome, long-term total parenteral nutrition (TPN) administration, systemic lupus erythematosus, ventriculoatrial shunts, congenital or acquired thrombotic tendencies, and acute deep venous thrombosis are all recognizable risk factors associated with PE in children.[21]

The clinical findings of PE in children are similar to those encountered in adults. However, none of these signs and symptoms is specific to establish the diagnosis of PE and could be associated with underlying co-morbid disease, reducing the level of suspicion by clinicians. In children,

individual symptoms and signs have low sensitivity and specificity for predicting a diagnosis of PE. Therefore, diagnosis of PE based on these signs and symptoms is difficult.[17-20]

The symptoms of PE in children may include shortness of breath, pleuritic chest pain, and hemoptysis. However, the clinical presentation may vary and may be subtle and mimic other diseases.[17] In adolescents, pleuritic chest pain is the most common presenting complaint, followed by dyspnea, cough, and hemoptysis.[21,22] Other signs and symptoms may include wheezing, rales, sweating, tachycardia, nausea, vomiting, syncope, murmur, and cyanosis. Pleurisy with friction rub may also be present.[21,22] In adults, clinical prediction rules based on clinical signs, symptoms, and risk factors have been published. In children, however, clinical prediction rules have not yet been validated.[21,22] Arterial blood oxygen is frequently reduced. However, normal blood gases do not exclude PE. The erythrocyte sedimentation rate is elevated in approximately 40% and electrocardiogram may show right ventricle strain.[21]

Chest X-ray is often normal in patients with pediatric PE. The signs including atelectasis, pleural effusion, elevated hemidiaphram, and infiltrate or consolidation are variable and not specific for PE.[21] Oligemia distal to PE (Westermark sign) or a shallow, wedged-shaped opacity with its base against the pleura (Hampton hump) are rarely seen.[21] CT pulmonary angiography (CTPA) can be performed quickly in critically ill patients. PE appears as filling defects in the pulmonary arteries. A normal helical CT scan reduces the probability of PE. The disadvantages of CTPA are the use of iodinated contrast and the presence of significant radiation exposure.[22] Stein et al. evaluated whether the radiation exposure could be decreased by safely increasing the use of ventilation-perfusion (V/Q) scanning and decreasing the use of CTPA using an imaging algorithm in which emergency department patients with a clinical suspicion of PE underwent chest radiography. If the chest radiograph was normal, V/Q scanning was suggested; otherwise, CTPA was recommended. The mean effective dose was reduced by 20%, from 8.0 mSv to 6.4 mSv ($p < 0.0001$) with no significant difference in the false-negative rate between CTPA and V/Q scanning.[23]

Radiopharmaceuticals and Imaging Technique

Perfusion Agent

The radiopharmaceutical used for lung perfusion imaging is ^{99m}Tc-macroaggregated albumin (^{99m}Tc-MAA). After slow intravenous injection in supine position, ^{99m}Tc-MAA particles lodges in pre-capillary arterioles, causing a temporary occlusion in a distribution proportional to regional arterial blood flow in lungs. The number of occluded arterioles by ^{99m}Tc-MAA particles is approximately 0.1% of their total number which is relatively small.[24] The particles clear by enzymatic hydrolysis and are eventually phagocytized by reticuloendothelial system and eliminated in the bile, with a biologic half-life in the lungs of between 6-8 hours. The particle size is generally between 10-90 μm (90% of particles), with an average number of 500,000 particles in adult dose. In children, the number of particles should be adjusted to the age or weight to keep the number of particles as low as possible in order to embolise no more than 0.1% of the total lung capillary vessels.[24] It is estimated that neonates have about 10% of the eventual number of adult pulmonary capillaries. The number of capillaries increases to half of the adult value by age 3 years, and reaches an adult level by age 8-12 . The number of injected particles should not exceed 50,000 in the newborn and 165,000 for 1 year old children. The recommended number of particles for 5-10 year olds with an average weight of 20-35 kg is from 200,000-300,000.[24] The recommended dose by North American Consensus Guidelines is 2.59 MBq/kg (0.07 mCi/kg) if ^{99m}Tc is used for ventilation study and 1.11 MBq/kg (0.03 mCi/kg) if no concomitant ^{99m}Tc ventilation study is performed, with a minimum dose of 14.8 MBq (0.4 mCi).[3,25] When administering ^{99m}Tc-MAA, withdrawing blood into the syringe should be avoided as small clots may occur with hot spots appearing on the images. If ^{99m}Tc-labeled radioaerosols or Technegas are used for ventilation scan, the scan should be performed first. If ^{81m}Kr gas is used for the ventilation scan, this can be acquired before or after the perfusion scan or both examinations may be performed simultaneously as a dual-isotope scan.[24,25]

Images can be acquired after radiotracer administration using a high-resolution, low-energy collimator. Planar images are obtained in a 128 × 128 or 256 × 256 matrix format, with a zoom large enough to include both lungs in the field of view with good margins. Multiple projections should be obtained including anterior, posterior, anterior and posterior oblique, and both lateral projections (Fig. 2). SPECT or SPECT/CT study can also be performed. The CT portion is acquired with a low dose CT for attenuation and anatomic correlation.[24,25]

Ventilation Agents

^{99m}Tc-DTPA Aerosol: ^{99m}Tc-DTPA aerosol is the most commonly used radiopharmaceutical. Many different aerosols have been used, but DTPA is preferred in children because of the fast renal clearance, which lowers the radiation burden. ^{99m}Tc sulfur colloid aerosol may be used but it has a slower clearance from the lungs.[24]^{99m}Tc-DTPA Aerosol can be inhaled through a mask connected to a nebulizer containing a saline solution of the radiopharmaceutical or preferably using a mouthpiece and nose clips in older children.[24] Swallowing of saliva may cause high gastric signal with possible difficult visualization of the left lower lung field.[24]Co-operative children can be asked to rinse their mouth with water before the beginning of the acquisition. Aerosolized Tc-DTPA crosses the alveolar-capillary membrane and enters the bloodstream where it is then filtered by the kidneys. Increased permeability of alveolar-capillary membrane and thus lung clearance can be seen after exercise or certain lung disease such as cystic fibrosis. The calculated administered dose is scaled on a body surface basis. Minimum activity within the lungs should be not less than 10 MBq, to allow for sufficient count statistics.[24]

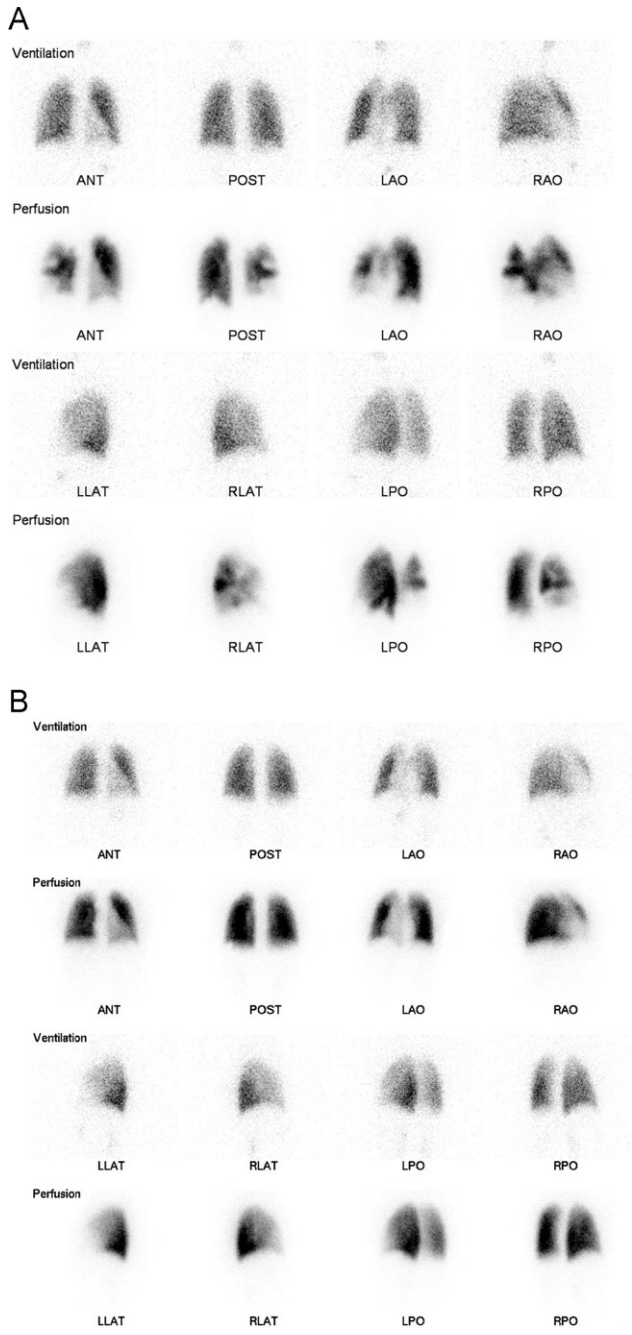

Figure 2 V/Q scan. (A) Multiple mismatched perfusion defects suggestive of the high probability of pulmonary emboli in a 16-year old girl with thrombotic thrombocytopenic purpura (TTP) and deep vein thrombosis (DVT). (B) V/Q scan 3 months after treatment.

Imaging is usually performed before perfusion imaging (Fig. 2). Because both agents are labeled with ^{99m}Tc, it is extremely important that the counting rate of the second study be at least 3 times the counting rate of the first study.[25] One advantage of ^{99m}Tc-DTPA Aerosol is the persistence of activity in the lungs which allows acquiring multiple projections or SPECT to match the perfusion images. Also, collection systems are not necessary as they are for radioactive gases.[24]

Xenon-133: Xenon is an inert gas with low solubility in body fluids and higher solubility in fat. After 133Xe inhalation in a single breath the pattern of distribution reflects the regional ventilation. It has a physical half-life of 5.24 days and a low energy gamma emission (81 keV). However, it rapidly washes out from the lungs with a half time of 5-30 seconds. The usual dose for children is 10-12 MBq/kg (0.3 mCi/kg) with a minimum dose of 100-120 MBq. The Xe-133 ventilation scan is generally performed prior to the Tc-99m MAA perfusion exam, as downscatter from the Tc-99m would severely degrade image quality. A posterior projection is generally used while a bolus of ^{133}Xe is injected into the mouthpiece of the spirometer system at a time when the patient begins maximal inspiration. The imaging room should provide appropriate exhaust for radioactive gas. The advantage of xenon exam is the ability to obtain single breath, equilibrium and washout images providing a better evaluation of ventilation and sensitivity for obstructive lung disease.[24]

^{99m}Tc-Technegas: Technegas consists of ultrafine particles of ^{99m}Tc labeled carbon clusters and produced by evaporating Tc-pertechnetate at very high temperatures of approximately 2500°C in a crucible in the presence of argon gas. The Tc-carbon particle is so small that it acts like a gas. The median size of the technegas particles is most likely between 30-60 nm. Technegas is inhaled via a face mask in a well ventilated room. There is good peripheral deposition with more homogeneous tracer distribution on SPECT study compared to 99mTc-DTPA aerosols, particularly in patients with obstructive airways disease. The inhalation may cause transient hypoxemia; this can be overcome by giving oxygen via nasal canula.[25]

Krypton-81m: ^{81m}Krypton gas is produced by a rubidium generator (^{81}Rb/^{81m}Kr) with a half life of 13 seconds and emission of a 190 KeV gamma ray. Gas is administered by continuous inhalation during the acquisition of the images, mixed with atmospheric air. Because it has a short half life, Krypton-81m is not considered an environmental hazard and storage or exhaust systems are not necessary. The radiation dose to the lungs is lower than with other agents. However, the generator is expensive and can be used only for 1 working day which makes it impractical for most clinical situations and currently is not available in the United States.[24,25]

Interpretation

Several diagnostic schemes have been suggested for interpretation of V/Q scans, such as the modified Prospective Investigation of Pulmonary Embolism Diagnosis (PIOPED) II with the proposed criteria for a very low probability interpretation to improve the accuracy and minimize the number of non-conclusive results.[26] However, in the daily practice of nuclear medicine, experienced physicians do not follow a strict single interpretive criteria but rather use integrated knowledge of different published criteria and their own experience ("Gestalt" interpretation).[27] Numerous studies were carried out to evaluate the performance of different readers with various experiences using several widespread

algorithms. Webber et al.[28] compared the PIOPED criteria with earlier schemes developed by McNeil and Biello and failed to demonstrate statistically significant difference among the different sets of criteria. However, the Biello criteria demonstrated the greatest area under the receiver operating characteristic curve and with fewer indeterminate results; therefore, the author suggested that the Biello scheme represents the best scheme among the sets of criteria studied. Hagen et al.[29] also reported a good accuracy and interobserver variability for PIOPED, Hull and Gestalt interpretation.

In general, the ideal scheme would minimize the frequency of intermediate or indeterminate results. However, the interpretation of a single moderate-sized segmental V/Q mismatch is still challenging and the significance of single segmental V/Q mismatch remains controversial. A varying prevalence of PE has been reported with such findings which reclassified into the intermediate probability in modified PIOPED similar to Biello criteria.[30] However, Stein et al.[31] showed that in patients with no underlying cardio-pulmonary disease, this finding has a PPV of 86% which puts the patient into the high probability category. Stein et al. also found fewer intermediate probability results in patients with normal chest X-ray. Therefore, stratification of patients may alter the probability and minimize the indeterminate results in a subgroup of patients. Recently, Glaser et al.[32] proposed a trinary interpretation for V/Q scanning which considered normal, very low probability, and low-probability read as no evidence of PE, high probability as PE present, and intermediate probability as non-diagnostic. They also consider single segmental mismatches to be positive for PE, consistent with Stein's result mentioned above. In their study, they compared this new scheme with the traditional probability interpretative strategy and reported similar outcomes with no statistically significant difference in false negative rates between the 2 interpretative schemes ($P = 0.63$). The trinary interpretation group included 664 examinations, with 8.4% being PE present, 3.5% nondiagnostic, and 88.1% PE negative. Pediatric subgroup analysis in 20 children showed positive in 10%, nondiagnostic in 5%, and negative in 85%, with no false negatives using either scheme. They concluded that the trinary interpretation can safely be used. In children, Gelfand et al. evaluated the frequency of indeterminate findings in children without known lung disease or previous extensive PE, and reported a low rate of indeterminate studies (15%) using criteria of Biello et al. with minimal modification. It was concluded that V/Q scan has less radiation dose than CTA and still appropriate for imaging children with suspected PE.[33]. In our institution the percentage of indeterminate/intermediate studies is 10%.

In summary, V/Q lung scan is easy to perform, even in small children, and still safely appropriate to carry out in children with suspected PE with less radiation exposure than CTPA. The indeterminate results in children and adolescents are low in the selected group with no known history of lung disease. Therefore, it is still appropriate to perform V/Q lung scan in children with suspected PE as a first imaging test in a hemodynamically stable patient with no history of lung disease and normal chest radiograph.

Meckel's Scan for Acute Lower GI Bleeding

Lower GI bleeding in infants and children is commonly seen in clinical practice. It may be caused by a variety of lesions among which are Meckel's diverticulum, intussusceptions, infectious enterocolitis, intestinal duplication, malrotation with volvulus, polyps, bleeding disorders, GI allergy, and inflammatory bowel disease. Meckel's diverticulum is one of the most common causes of lower GI bleeding and the most common cause in infants, and occurs in 1%- 3% of population.[2] This congenital abnormality arises from the antimesenteric side of the ileum, representing incomplete closure of the omphalomesenteric duct. It is most likely located approximately 90 cm proximal to iliocecal valve. Usually, it contains ileal mucosa but may contain variable ectopic mucosa and the most commonly ectopic tissue seen is gastric mucosa, which is seen in 10%-30% of cases and 60% of symptomatic patients as well as in almost all of the patients with bleeding.[2] The most common symptom is painless bleeding; however, it may be associated with abdominal pain. The bleeding is caused by mucosal ulceration of the Meckel's diverticulum or adjacent ileum due to hydrochloric acid secretion from ectopic gastric mucosa within the Meckel's diverticulum. ^{99m}Tc pertechnetat scintigraphy (Meckel's scan) is the best noninvasive procedure to establish the diagnosis of ectopic gastric mucosa in Meckel's diverticulum[2]

Radiopharmaceuticals and Imaging Technique

The recommended dose is 1.85 MBq/kg (0.05 mCi/kg) with a minimum dose of 9.25 MBq (0.25 mCi) and maximum dose of 370 MBq (10 mCi) injected intravenously after fasting for approximately 4 hours.[3] Detection of ectopic gastric mucosa in Meckel's diverticulum may be improved by certain premedication. Histamine H2-receptors antagonists, such as Cimetidine inhibits secretion of pertechnetate by gastric mucosa without affecting the uptake. Ranitidine can also be used with a dose of 1 mg/kg given intravenously over 20 minutes 1 hour before the test. Pentagastrin increases the uptake in gastric mucosa. It is injected subcutaneously prior to tracer administration with a dose of 6 μg/kg. Glucagon decreases peristalsis of the GI tract; however, it decreases tracer uptake in the gastric mucosa and should be used in conjunction with Pentagastrin. Perchlorate can suppress the gastric mucosa and should be avoided.[2,34] Imaging can be started immediately after the injection in supine position using high resolution collimator. Early dynamic images can be obtained to assess for vascular malformation and possibly to detect the site of bleeding. A flow study for 1 minute is obtained followed by continuous imaging (1 min/frame) for 30 minutes in anterior projection. Delayed static images can also be acquired, if needed. Lateral images can be helpful to differentiate a Meckel's diverticulum located anteriorly from urinary activity which is normally localized posteriorly.[2] The intense urinary bladder activity may obscure some Meckel's diverticulum uptake if located adjacent to bladder and routine

post-void imaging is recommended. Some have suggested that SPECT imaging can also be used.[2,34]

Interpretation

The typical finding for Meckel's diverticulum is a well-defined focus of an increase in uptake, most frequently in the right lower quadrant, anteriorly visualized simultaneously with gastric uptake (Fig. 3). The uptake usually persists and increases over the time. Rarely, the activity may vary due to intestinal secretions or hemorrhage. The accuracy of Meckel's scan is 90% in surgically proven patients with overall sensitivity of 85% and specificity of 95%.[35] There are several abnormalities which may demonstrate increased uptake and cause false positive results, including duplication cysts or enteric duplication containing ectopic gastric mucosa, intestinal obstruction, intussusception, inflammation, ulcers, and vascular tumors (Fig. 4). In addition retained activity in renal pelvis or collecting system may also cause a false positive result.[34] Low uptake of gastric mucosa in infants may cause a false negative. However, extending the imaging time by up to 1-2 hours may increase the ability to detect a lesion with lower background activity (Fig. 4) [2]. False negative may result from residual barium from a prior study or from the small size of ectopic gastric mucosa in Meckel's diverticulum.

^{99m}Tc-RBC

^{99m}Tc-red blood cell (^{99m}Tc-RBC) scintigraphy generally is useful for assessing lower GI bleeding in patients from any cause including Meckel's diverticulum.[36] One of the advantages of using ^{99m}Tc-RBCs is that it remains intravascular allowing a longer imaging time over the course of several hours and the possibility to detect intermittent bleeding.[36,37] Bleeding rates as low as 0.1-0.4 mL/min may be detected.[37]

Radiopharmaceuticals and Imaging Technique

Labeling of RBCs with ^{99m}Tc by the in vitro method provides the highest efficiency which is recommended and widely used. The disadvantage of lower labeling efficiencies using in vivo or modified in vivo methods is the possible secretion of free pertechnetate within the gastric mucosa into the duodenum and also excretion of free pertechnetate into the urinary collecting system, increasing the possibility of false positive results.[36] The recommended dose is 7.4 MBq/kg (0.2 mCi) with maximum dose of 740 MBq (20 mCi).[37] After injection, flow study is acquired for 60 seconds (1 s/frame) followed by dynamic imaging for 60-120 minutes. Additional delayed images can be obtained, if necessary.[37]

Interpretation

Bleeding sites can be detected by extravascular accumulation of tracer activity with antegrade or retrograde motion of tracer along the bowel lumen.[36,37] The motion is best detected on cinematic display and may occur very rapidly. Small bowel bleeding may be distinguished from a colonic source by the demonstration of rapid distal progression through a series of multiple, small, centrally located, curvilinear segments on cinematic display of the abdomen. Large bowel bleeding has a more elongated pattern with peripheral location within the abdomen compared with bleeding within small bowel.[36]

Alternatively, ^{99m}Tc-sulfur colloid can also be used to evaluate lower GI bleeding. High bleeding to background activity ratio can be achieved which allows detecting rates as low as 0.05-0.1 mL/min. However, dynamic imaging is obtained for approximately 30 minutes which limits the possibility to detect intermittent bleeding. In addition, the high tracer accumulation in the liver and spleen may obscure adjacent bleeding activity sites.[36,37]

Hepatobiliary Scintigraphy

Cholecystitis is less common in children than in adults but the incidence in children is believed to be increasing. It is more common in adolescent girls than boys. Acute cholecystitis is associated with inflammation in the wall of the gallbladder.[36,38] In acute calculous cholecystitis, the cystic duct is obstructed by gallstones. Accumulated mucus causes increased pressure and gallbladder distension, edema, and bile stasis, leading to bacterial overgrowth. Cholecystitis with underlying cholelithiasis is more common in children with hemolytic anemia.[36] In acute acalculous cholecystitis, inflammation occurs in the absence of gallstone. Usually it is associated with sepsis, infections such as Streptococcal infections, vasculitis such as Kawasaki's disease, trauma, malignancy, and metabolic or congenital diseases. It may occur in TPN or following surgery.(36) These conditions allow the formation of biliary sludge. Biliary sludge may then cause a cystic duct obstruction. The associated inflammation and edema may compromise blood flow and lead to bacterial infection. Acalculous cholecystitis is not common; however, it is relatively more frequent in children than adults.

Generally, children present with abdominal pain localized in the right upper quadrant or epigastric region. Other symptoms include nausea, vomiting, anorexia, and fever for several days. On physical examination,a right upper quadrant tenderness is the most common finding. Jaundice may be present. The gallbladder may be enlarged and palpable. Leukocytosis is a common finding.[36,38] Ultrasound is essential for evaluating the biliary tract and detecting gallstones. However, its diagnostic accuracy has a substantial margin of error.[39] Findings could include stone visualization, obstruction of the neck of gallbladder, wall thickness, local tenderness over the gallbladder (radiologic Murphy sign), gallbladder distension and surrounding fluid accumulation.

Hepatobiliary scintigraphy is the most accurate diagnostic imaging modality for acute cholecystitis. Recently, Kiewiet et al.[39] reported a systematic review of different imaging modalities in patients with suspected acute cholecystitis. In this review, 57 studies were included. The sensitivity and specificity for hepatobiliary scintigraphy were 96% and 90%. The sensitivity of hepatobiliary scintigraphy was significantly higher than ultrasound (81%).

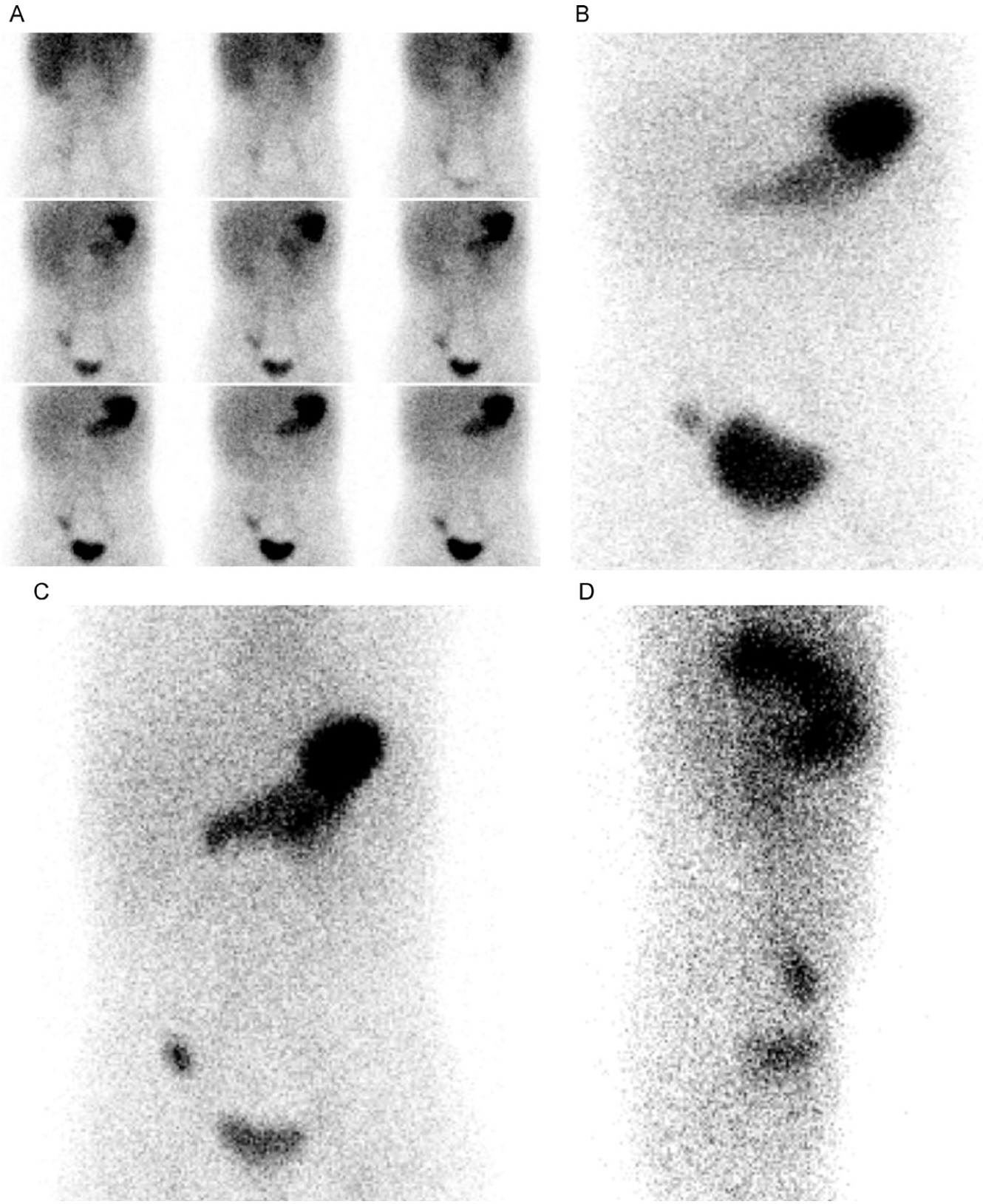

Figure 3 Meckel's diverticulum. A 2-year old boy with bloody stools. (A) Sequential dynamic images show focal uptake in the right lower quadrant visualized at a rate similar to the gastric uptake. Delayed images at 45 minutes before (B) and after voiding (C) has been done to exclude any possible activity in the ureter. Left lateral view (D) shows that the activity is located more anteriorly. The diagnosis of Meckel's diverticulum confirmed at surgery.

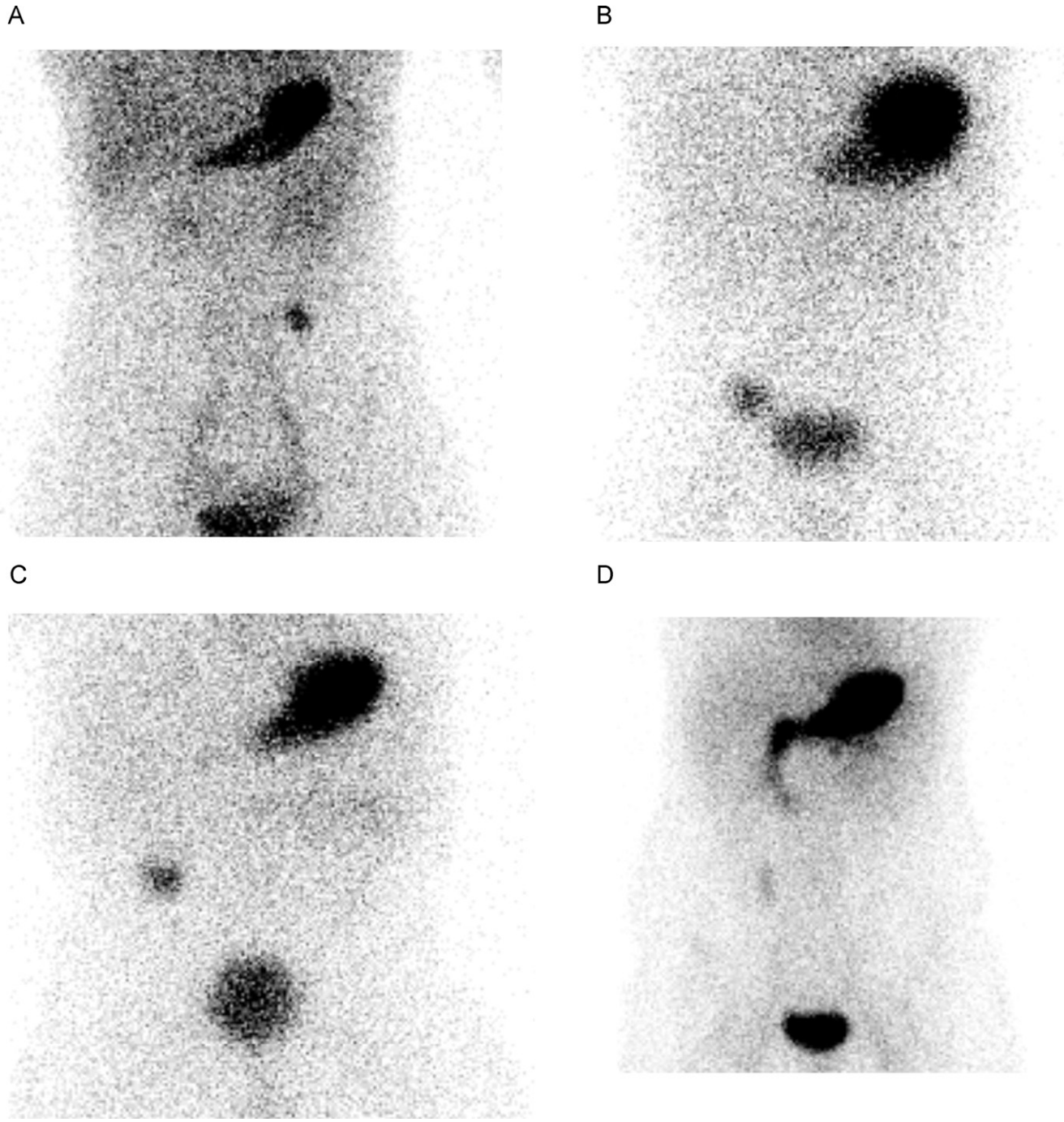

Figure 4 (A) Delayed view at 30 minutes in a 15-year old girl with GI bleeding showed a focal uptake in the left lower quadrant confirmed at surgery to be a Meckel's diverticulum. (B) Delayed view at 45 minutes in an 8-year old girl showed focal increased activity in the right lower quadrant. Earlier images up to 30 minutes did not identify any focal increased activity (not shown). The focal increased uptake moved more superiorly at 60 minutes (C). The diagnosis of Meckel's diverticulum confirmed at surgery. (D) A focal uptake is first visualized at 45 minutes in the right lower quadrant in a 9-year-old girl. The diagnosis of a duplication cyst with ectopic gastric mucosa was confirmed at surgery.

^{99m}Tc-disofenin or ^{99m}Tc-mebrofenin is administered intravenously.[40] The administered activity for infants and children is 1.85 MBq/kg (0.05 mCi/kg), with a minimum administered activity of 18.5 MBq (0.5 mCi). Mebrofenin is always preferred in jaundiced infants with hyperbilirubinemia, with a minimum administered activity of 37 MBq (1.0 mCi), as up to 24-hour delayed images are often required. The patient should be fasting for 4 hours prior to the test. Immediately after the injection, dynamic imaging is acquired for 60 minutes (0.5-1 min/frame) in anterior projects using preferably a high-resolution collimator and 128 × 128 matrix. Additional views such as right lateral, left or right anterior oblique may be performed, if required. When acute cholecystitis is suspected and the gallbladder is not seen within 60 minutes, delayed images for up to 4 hours should be obtained.[40]

Acute cholecystitis is associated with nonvisualization of the gallbladder on hepatobiliary scintigraphy and visualization of gallbladder activity excludes the diagnosis of acute cholecystitis in adults with high accuracy. However, in children, visualization of the gallbladder does not entirely exclude cholecystitis as gallbladder visualization, though infrequent, is possible in acalculous cholecystitis.[36] If the gallbladder is visualized after the initial 60-minute images and does not significantly empty, additional dynamic imaging for 60 minutes is acquired following infusion of 0.02 μg/kg sincalide, a synthetic C-terminal octapeptide of cholecystokinin. Poor contraction and emptying of the gallbladder following sincalide may occur in partial cystic duct obstruction, acalculous cholecystitis or chronic cholecystitis. As in the case of adults, morphine augmentation of hepatobiliary scintigraphy of acute cholecystitis may help reduce the number of false positive studies in children and reduce scanning time; however, in acute acalculous cholecystitis, it may overcome functional obstruction of the cystic duct resulting in a false negative examination.[36]

Hepatobiliary scintigraphy in children can also be used for the evaluation of choledochal cyst and biliary leak. In infants, hepatobiliary scintigraphy is used to differentiate biliary atresia from hepatocellular disease.[2] Premedication with phenobarbital (5 mg/kg/d) for 3-5 days before hepatobiliary scintigraphy increases bile secretion and improves the diagnostic differentiation between biliary atresia and neonatal hepatitis.[40] Hepatobiliary scintigraphy after phenobarbital therapy is highly accurate for differentiating biliary atresia from other causes of neonatal jaundice. Hepatobiliary scintigraphy has 97% sensitivity and 82% specificity (91% accuracy) in the diagnosis of biliary atresia.[2] Ursodeoxycholic acid has also been included in the pre-treatment regimen to stimulate bile secretion.[40] Hepatobiliary scintigraphy can exclude the diagnosis of biliary atresia by identifying the biliary drainage of the radiotracer into the bowel. If no bowel activity is detected up to 24 hours and liver uptake is normal, the diagnosis of biliary atresia is suspected.[2] However, normal liver uptake of tracer with no excretion up to 24 hours can occur in severe cases of neonatal hepatitis, Alagille syndrome, dehydration, sepsis, TPN cholestasis, and bile plug syndrome in cystic fibrosis. Neonatal hepatitis typically demonstrates reduced hepatocyte uptake and delayed hepatobiliary transit of tracer into the bowel.[36]

Renal Cortical Imaging for Pyelonephritis

Urinary tract infection (UTI) is relatively a common infectious disease in children. Usually, it is ascending in origin and is caused by perineal contaminants.[41] However, in neonates, infection can be hematogenous in origin which may explain the nonspecific symptoms associated with UTI in these patients. The infection is called lower-tract infection when it is limited to urinary bladder (cystitis) and upper tract infection when renal paranchyma is involved (pyelonephritis). The prevalence of pyelonephritis varies by age and sex. About 60%-65% of children with febrile UTIs have acute pyelonephritis, as defined by presence of abnormalities of the renal cortex on ^{99m}Tc-dimercaptosuccinic acid (^{99m}Tc-DMSA) scan.[42] *Escherichia coli* are the most common organism, and the cause of more than 90% of acute pyelonephritis cases. The incidence of renal scarring following acute pyelonephritis varies by region from 26.5%-49%.[42]

In pediatric patients, it may be very difficult to differentiate pyelonephritis from cystitis, based on clinical symptoms and the presentation may vary with age.[2] Children may present with fever, flank pain, vomiting, malaise, irritability, leukocytosis, and bacteriuria. Neonates and infants may have nonspecific clinical presentation.[2,41] Early recognition and prompt treatment is important to prevent late complications such as renal scarring, hypertension, and renal failure.[41]

Renal ultrasonography is useful to exclude congenital malformations and hydronephrosis, as well as to assess the size and shape of kidneys. However, it has low sensitivity in detecting acute pyelonephritis.[43] In addition, renal ultrasonography is less sensitive than ^{99m}Tc-DMSA scan in detecting renal scar. Temiz et al.[44] showed that, irrespective of the reflux grade, ^{99m}Tc-DMSA scan detected scars in 35% of the kidneys reported to be normal on ultrasound.

Radionuclide Cystography or Voiding cystourethrography are helpful for evaluating the bladder and detecting vesicoureteric reflux. However, pyelonephritis may occur with the absence of reflux, thus limiting the renal cortical evaluation in UTI to only children who have vesicoureteric reflux is not advised.[45] Recently, some investigators suggested a so called top-down approach with a ^{99m}Tc-DMSA scan as the first line study instead of a radionuclide cystography because of the relative importance of renal damage rather than reflux in these patients.[46]^{99m}Tc-DMSA scintigraphy is considered the most reliable, simplest, and most sensitive method for the early diagnosis of focal or diffuse functional cortical damage.[2] This test can identify the degree of renal damage and assess recovery of function after treatment. The high sensitivity of ^{99m}Tc-DMSA scintigraphy for the diagnosis of pyelonephritis is well established. Sensitivity is 96%, and specificity is more than 98%.[2]^{99m}TC-DMSA renal scan is also useful to evaluate ectopic kidney, horseshoe kidney, assessment of the functioning cortical tissue in a dysplastic or small kidney, and differential renal function.

Radiopharmaceuticals and Imaging Technique

The radiotracer of choice for evaluation of the renal cortex is ^{99m}Tc-DMSA. The tracer is taken up by the proximal tubular cells, directly from the peritubular vessels with 40%-65% of the injected dose present in the cortex 2 hours after the injection.[2] Only 10% is excreted into the urine within 2 hours. The greater amount of activity in the cortex and lower excretion produce excellent renal cortical imaging without interference from urinary activity.

Alternatively, ^{99m}Tc-Glucoheptonate can be used for renal cortical imaging with 10%-20% of the injected dose present in the proximal convoluted tubules of the cortex 2 hours after injection.[47] However, retained activity in the pelvicalyceal

system may interfere with renal cortex assessment and may cause misinterpretation especially for children with a history of renal obstruction. Furosemide, hydration, and delayed imaging could be considered in patients with hydronephrosis.

The recommended dose for ^{99m}Tc-DMSA is 1.85 MBq (0.05 mCi)/kg with a minimum dose of 18.5 MBq (0.5 mCi) injected intravenously.[3]

Planar images can be obtained 2-4 hours after the administration of the radiotracer when the background activity is minimal.[2,45] Delayed images can be performed in patients with reduced renal function or delayed clearance. Planar images are used to evaluate the position and the configuration of the kidneys as well as the differential renal function. In addition, it is recommended that pinhole images be obtained in younger children. Pinhole images provide higher resolution than planar images to detect cortical defects in younger children.[2] SPECT study can be performed in older children. SPECT study is superior to planar imaging for evaluation of the renal cortex and can detect more defects than planar images. Although SPECT is better in defining the location of the lesions, it has only a marginal increase in sensitivity. Mouratidis et al.[48] evaluated 41 children and found more defects detected by SPECT than planar imaging (24 vs 20) but with no statistically significant difference. The authors concluded that although the risk of missing renal cortical defects is low when using high-resolution planar images, SPECT should be performed whenever feasible. Applegate et al.[49] found similar result with more affected kidneys detected by SPECT and concluded that SPECT is superior to planar imaging for demonstrating renal cortical defects. Recently, Brenner et al.[50] found no statistically significant difference in the average number of abnormal segments detected by planar (2.1) vs SPECT imaging (2.2).

Interpretation

The activity distribution in ^{99m}Tc-DMSA images demonstrates the configuration of renal cortex. The contour of normal kidneys is generally round and regular with no uptake in the medulla and pelvicalyceal system; however, variable shape of the renal contours can be seen. Flattening of the lateral aspect of the upper left kidney due to splenic impression or indentations in the contour of the kidney due to fetal lobulation are normal variants. External attenuation may also mimic a cortical defect. Poles may appear relatively hypoactive in contrast with underlying hyperactive columns of Bertin, giving a false impression of a polar lesion.[45] On SPECT study, interrenicular septum may cause a linear area of absent uptake extending from the renal hilum into the renal parenchyma and may be confused with scar.[51] The normal differential renal uptake is between 45%-55%.[2]

Acute pyelonephritis appears as a single or multifocal area of decrease in cortical uptake of ^{99m}Tc DMSA without volume loss (Fig. 5). Less frequently, it may present as a diffuse decrease in radiotracer activity with kidney enlargement.[2,45] Renal scar is usually associated with volume loss and more defined edges. Cortical abnormalities after an acute pyelonephritis may resolve over several months or may lead to a permanent scar formation. Decreased cortical uptake without deformity of the contour is likely to resolve over

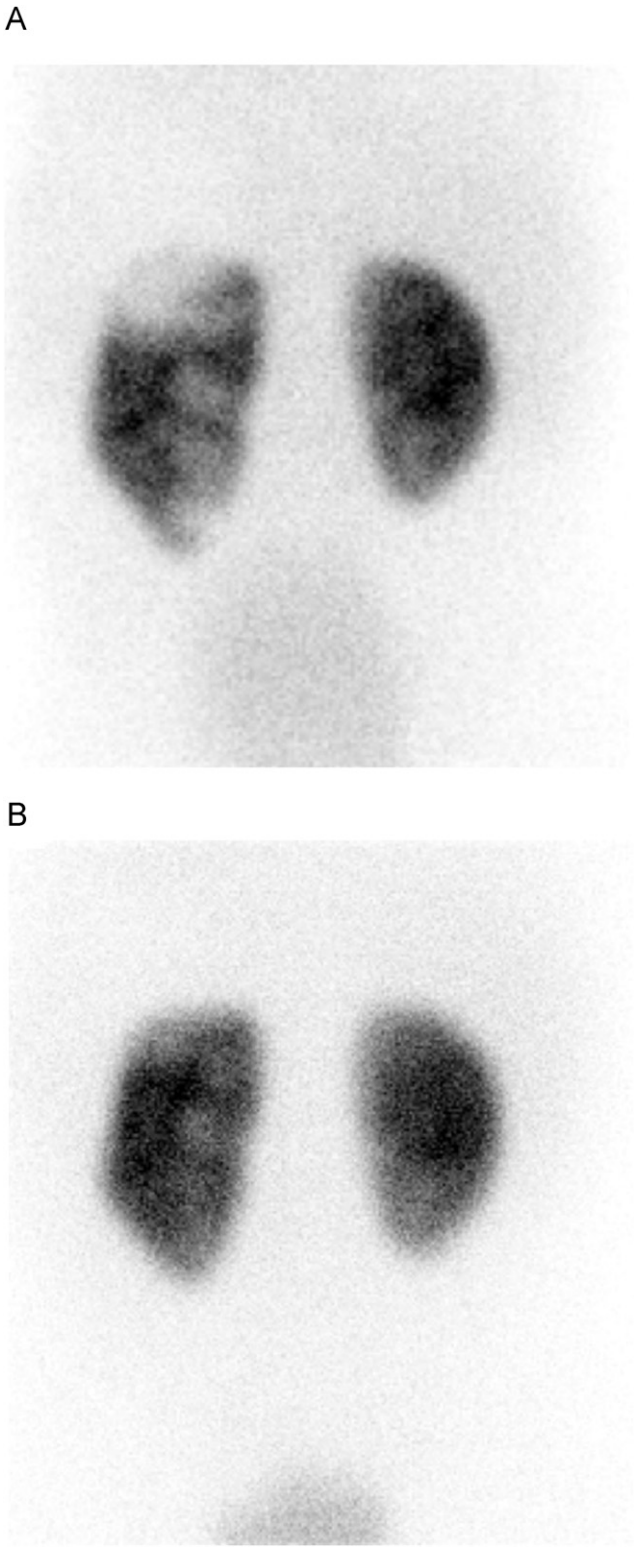

Figure 5 Acute pyelonephritis. (A) Posterior pinhole image with ^{99m}Tc-DMSA in a 2-year old girl shows multiple areas of decreased cortical uptake in the upper and lower poles. (B) Follow up posterior pinhole image obtained 6 months later after therapy shows resolution of most defects.

several months, whereas deformed contour often corresponds to renal sequelae.[45] A follow-up ^{99m}Tc-DMSA study at least 6 months after acute pyelonephritis may be useful to detect scarring.[45,47]

Renal Transplant

Renal scanning is used early and late after renal transplantation in children to evaluate the effectiveness of the transplant surgery and detect complications. Usually, a baseline renal scan is performed in the first 24-72 hours post-transplantation if no surgical complications are suspected and blood pressure and creatinine are as expected. Follow-up studies can be performed, depending on the patient's condition.[52]

^{99m}Tc-mercaptoacetyltriglycine (^{99m}Tc-MAG3) is the agent of choice for dynamic renal scintigraphy and can effectively evaluate renal function, urine drainage, and renal transplant allograft. After intravenous injection, ^{99m}Tc-MAG3 is cleared mainly by active tubular cell transport. The extraction fraction of MAG3 is better than that of DTPA, resulting in higher initial renal uptake and a higher kidney-to-background ratio.[52] The usual administered dose of ^{99m}Tc-MAG3 is 3.7 MBq (0.1 mCi)/kg, given intravenously. If a flow study is required, the recommended dose is 5.55 MBq/kg (0.15 mCi/kg), with a minimal dose of 37 MBq (1.0 mCi) and maximum dose of 148 MBq (4 mCi).[3] Flow study is acquired immediately after injection for 60 seconds (1 s/frame) followed by dynamic imaging in an anterior position for 20-30 minutes. Delayed and oblique images can be performed, if required. Early after surgery, a normal scan of the transplanted kidney, mainly from live donors, demonstrates normal flow, uptake, and transit time. Acute tubular necrosis may occur predominantly in renal transplant from deceased donors and ^{99m}Tc-MAG3 images demonstrate parenchymal retention of the tracer with minimal or no activity in the renal collecting system. In acute rejection, the transplanted kidney has decreased perfusion and poor uptake on ^{99m}Tc-MAG3 scan. Urinary leak usually occurs during the first few months after renal transplant. It can be detected by renal scintigraphy, which shows a focal or diffuse area of increased activity in the abdomen outside the margins of the transplanted kidney, ureter, and bladder.[52]

Bone Scintigraphy

^{99m}Technetium-methylene diphosphonate (^{99m}Tc-MDP) is the most commonly used radiopharmaceutical for bone scintigraphy. This tracer concentrates in the amorphous calcium phosphate and crystalline hydroxyapatite reflecting both blood flow and osteoblastic reaction of bone. The recommended dose for children by North American Consensus Guidelines is 9.3 MBq/kg (0.25 mCi/kg) with a minimum dose of 37 MBq (1.0 mCi).[3] Other radiopharmaceuticals are also useful in evaluation of musculoskeletal disease such as ^{67}gallium-citrate (^{67}Ga) or labeled leukocytes using ^{111}In or ^{99m}Tc for musculoskeletal infection or a scan using ^{99m}Tc-sulfur colloid for bone marrow infarction particularly in sickle cell disease.[1,53]

PET imaging using ^{18}F-sodium fluoride (NaF) is being explored as an alternative to bone scintigraphy with ^{99m}Tc-MDP. It offers better sensitivity by improving the spatial resolution as PET scanner has greater ability than gamma camera to image high-energy photons of ^{18}F-NaF with similar radiation dosimetry.[54,55] In addition, scanning can be acquired as early as 30 minutes after injection, reducing the time of the study compared to bone scintigraphy using ^{99m}Tc-MDP.

Imaging Technique

Bone scintigraphy may include blood flow, blood pool and delayed imaging, which is called 3-phase imaging.[1,53] One of the most common indications for performing a 3-phase imaging in pediatric patients is osteomyelitis. Blood flow study is obtained immediately after radiotracer injection for 1 minute followed by blood pool images. Skeletal phase or delayed images are performed 2-4 hours later. Magnification technique with pinhole collimation improves resolution and can be particularly helpful in imaging small bony structures such as the femoral capital epiphysis. SPECT can improve the sensitivity and specificity of planar images and provide better anatomic localization. Generally, SPECT studies are superior to planar images and particularly useful in evaluation of back pain.[54,55] Combining the functional imaging of SPECT with the anatomic imaging of CT can further improve diagnostic accuracy and localization. Recently, SPECT/CT imaging systems have become available and are rapidly emerging as a useful technique in musculoskeletal imaging. In adult patients, SPECT/CT may be used for localization of osteomyelitis, inflammation, and both benign and malignant bone disease. Potential applications in children may include back pain and evaluation for suspected spondylolysis or enthesitis in the spinous processes.[55,56]

The normal distribution in pediatric bone scan may differ from adults.[55] In children, there is high physeal and apophyseal uptake due to rich blood supply and active enchondral ossification. Absence of uptake in nonossified cartilaginous structures should not be mistaken for avascular necrosis. Regions where this may be of concern in younger children include the femoral capital epiphysis, patella, and navicular bone. Before ossification, the ischiopubic synchondrosis appears as a discontinuity of the inferior pubic ramus. During ossification, increased uptake in ischiopubic synchondroses is a common normal variant and should not be misinterpreted as a pathologic lesion.[53]

Clinical Application

Acute osteomyelitis is a common pediatric disease that can occur at any age, most often affecting children younger than 5 years. Usually, it is the result of hematogenous spread of infection due to the rich vascular supply of the growing skeleton. It can be seen following direct puncture or spread of

infection from contiguous structure.[57] *Staphylococcus aureus* is the most common pathogen followed by streptococcus. Gram-negative bacteria and group B streptococci are frequently seen in newborns. *Salmonella* is an important cause of osteomyelitis in children with sickle cell disease.[57] Circulating organisms tend to infect the metaphyseal ends of the long bones, especially in the lower extremities, because of the high vascularity and sluggish circulation of the metaphyseal capillary loops. The femur, tibia, and humerus are most commonly affected. The presence of transphyseal vessels extending between the metaphysis and the epiphysis makes children less than 18 months of age particularly prone to septic arthritis of the adjacent joint. In older children, the growth plate is a relative barrier to the spread of infection into the epiphysis. Osteomyelitis in flat bones such as ilium and vertebrae are less frequent than long bones.[53] Limping or refusal to bear weight is often the only symptom in older children.[58] Radiography may be normal or only show deep soft tissue swelling within 48 hours of infection. Radiolucencies or periosteal reaction can be seen 7-10 days after infection.[57] However, many cases do not have the obvious plain film evidence of infection until 3-4 weeks.[59]

Three-phase bone scintigraphy is highly sensitive for the diagnosis of osteomyelitis. Typically, bone scans become positive 24-72 hours after the onset of infection. The sensitivity of 3-phase bone scan has been estimated as 94% with specificity of 95%.[60] Ideally, the bone scan should be obtained before joint aspiration. However, diagnostic aspiration and antibiotic therapy should not be delayed until the bone scan is completed, as fine-needle aspiration does not alter bone scan findings nor does antibiotic therapy lead to a rapid change in a bone scan.[53] A delayed whole-body scan on skeletal phase should be obtained as osteomyelitis in children can be multifocal or present with referred pain. In addition, malignant disease such as leukemia and sarcoma may mimic acute osteomyelitis.[53,54] Blood flow, blood pool, and delayed images show focally high uptake in the affected bone (Fig. 6). Occasionally, the affected bone in children shows low uptake or photopenic defect (cold osteomyelitis).[61] This is most likely due to reduced tracer delivery by increased intraosseous pressure from inflammation, edema, and joint effusion. Cellulitis can be differentiated from osteomyelitis as it typically demonstrates diffuse increased activity in the soft tissues on the dynamic and blood pool images, without focal osseous abnormality on delayed images.[59]

Septic arthritis is more common in children younger than 3 years . Monoarticular involvement is the most common pattern. The most commonly involved joints are the hip and knee. Clinical findings include fever, pain, swelling, and erythema of the involved joint. Pain with passive motion is the most consistent finding in septic arthritis. The most common infecting organism for septic arthritis is *S. aureus*. Transient synovitis is the most common condition that mimics septic arthritis. It is usually seen in children less than 10 years old and typically preceded by a upper respiratory viral infection. Transient synovitis is a self-limited condition that mostly involves the juvenile hip. It may be clinically indistinguishable from septic arthritis and joint aspiration is often required.

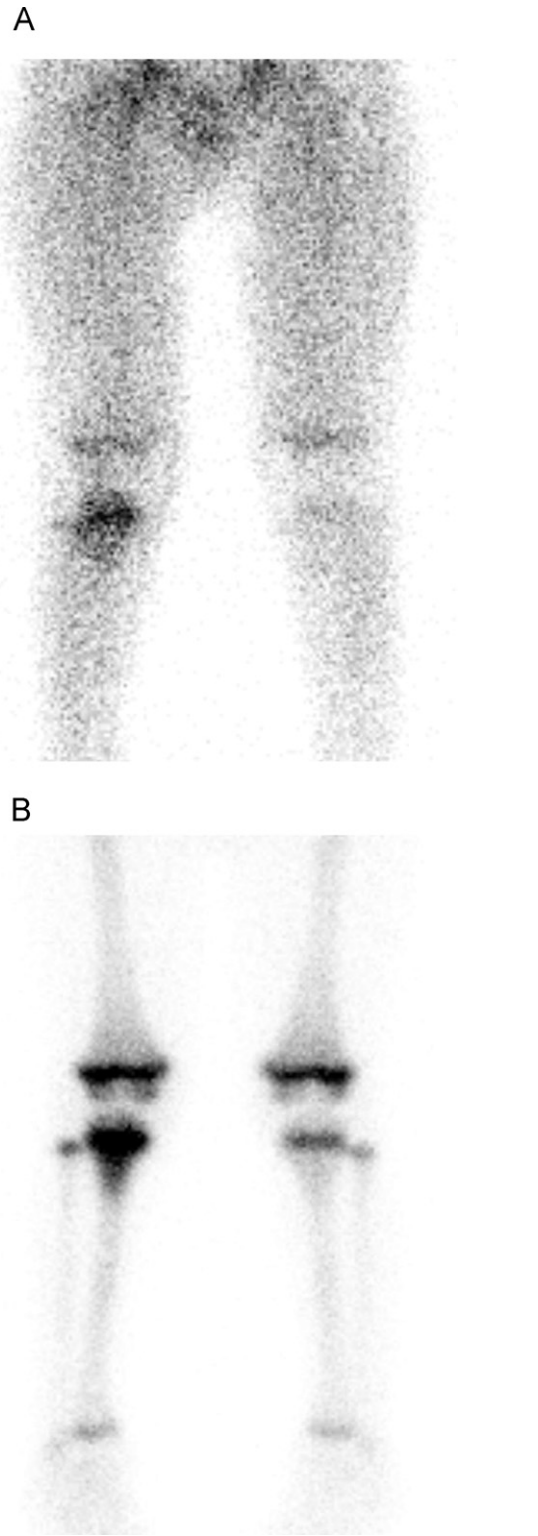

Figure 6 Acute osteomyelitis. Blood pool study (A) showed increased activity in the proximal right tibia. On delayed view (B) increased activity was localized in the proximal right tibia. Radiography was negative.

Early plain film evaluation of septic arthritis may demonstrate the presence of a joint effusion with joint space widening, subluxation. Ultrasound can identify joint effusion. Echogenic material within the effusion suggests septic arthritis.

Figure 7 Toddler's fracture. Diffusely increased uptake is noted in the left tibial diaphysis in a 20-month old boy with 8 days of pain and inability to walk after a fall.

In transient synovitis, the 3-phase bone scan may be normal or can demonstrate diffuse increased flow and blood pool activity. Delayed images may demonstrate increased periarticular activity in the affected joint. If a bone scan is performed before joint aspiration, decreased tracer uptake on delayed images may be seen as a result of vascular compression by the joint effusion. The proper course of action is to aspirate the joint promptly. Generally, bone scan is obtained after aspiration to detect any associated osteomyelitis.[54,58]

Legg-Calvé-Perthes disease is idiopathic ischemic necrosis of the femoral head in children. This disorder is most commonly seen in children between the ages of 5-8 years.[53] Patients typically present with pain in the affected hip and limping. Complications include premature osteoarthritis, osteochondritis dissecans. Diagnosis can be established by radiographs or magnetic resonance imaging (MRI). Bone scintigraphy is more sensitive than radiography for early diagnosis and is comparable to MRI.[54] In children, pinhole images should be routinely performed to improve resolution. Generally, early studies performed after the onset of clinical symptoms show absence of activity in the capital femoral epiphysis and can precede radiographic manifestations.[58] Later scans may demonstrate increased activity due to revascularization and remodeling. Conway's group demonstrated the prognostic value of bone scintigraphy.[62,63] They found that the persistent absence of bone uptake in the proximal femoral epiphysis after 5 months or metaphyseal hyperactivity is highly correlated with more severe disease and poorer prognosis. The early formation of a lateral column of tracer uptake in the capital femoral epiphysis, even before radiography, is associated with a good prognosis due to early revascularization. Later, Comte et al.[64] confirmed the early prognostic value reported by Conway's group and proposed using bone scintigraphy in routine management to identify patients at high risk for poor outcome.

Children with sickle cell disease frequently present to the emergency department with musculoskeletal pain. Bone scintigraphy usually demonstrates multiple sites of abnormal localization due to previous bone infarctions (Fig. 6). The challenge is to differentiate sickle cell crisis with possible bone marrow infarction from osteomyelitis.[53] Bone marrow scan with ^{99m}Tc-sulfur colloid in conjunction with bone scan can be used in evaluation of sickle cell disease. After the early onset of pain during a vasoocclusive crisis, if the bone marrow scan is abnormal at the site of pain followed by a normal or decreased uptake on bone scan, infarction is the likely diagnosis. Increased uptake in the blood pool and delayed images on bone scan is more suggestive of osteomyelitis.[1] In 1 series of 70 cases, bone infarction was diagnosed in 66 children with painful crises based on decreased uptake on bone marrow scan and abnormal uptake on bone scan without false-negative results. The other 4 patients had normal bone marrow scan and abnormal uptake on the bone scan suggestive of osteomyelitis.[65] When the bone scan is obtained more than 7 days after the pain onset, it may not be helpful in differentiating infarction from osteomyelitis. Gallium scan combined with a bone scan can be used. However, the use of gallium scans leads to significant radiation exposure.[1,66]

Generally, skeletal trauma can be evaluated by radiography. However, some injuries may be occult and bone scintigraphy can help localize the abnormality and assist in diagnosis. Bone scintigraphy is highly sensitive and becomes abnormal as early as a few hours after injury.

A toddler's fracture is a spiral or oblique fracture that most commonly involves the tibiae. Radiographic findings are often subtle and fractures may not be apparent. Bone scintigraphy is a valuable tool for detecting the injury early before radiographic changes are present. Typically, the bone scan shows diffuse increased uptake in the tibial diaphysis (Fig. 7). A linear or spiral pattern of high uptake may be seen in some children.[1,53]

Stress injury occurs due to repetitive stress on normal bone causing internal remodeling that involves osteoclastic resorption and osteoblastic repair. Stress fractures can occur when resorption exceeds bone replacement which temporarily weakens the cortex.[66] Bone scintigraphy is more sensitive than radiographs in detecting stress fractures. The bone scan is usually abnormal at the time of presentation and can precede plain film changes by up to a few weeks.[67] MRI can be used in stress injury[68]; however, the advantage of bone scintigraphy is that the entire skeleton can be screened.

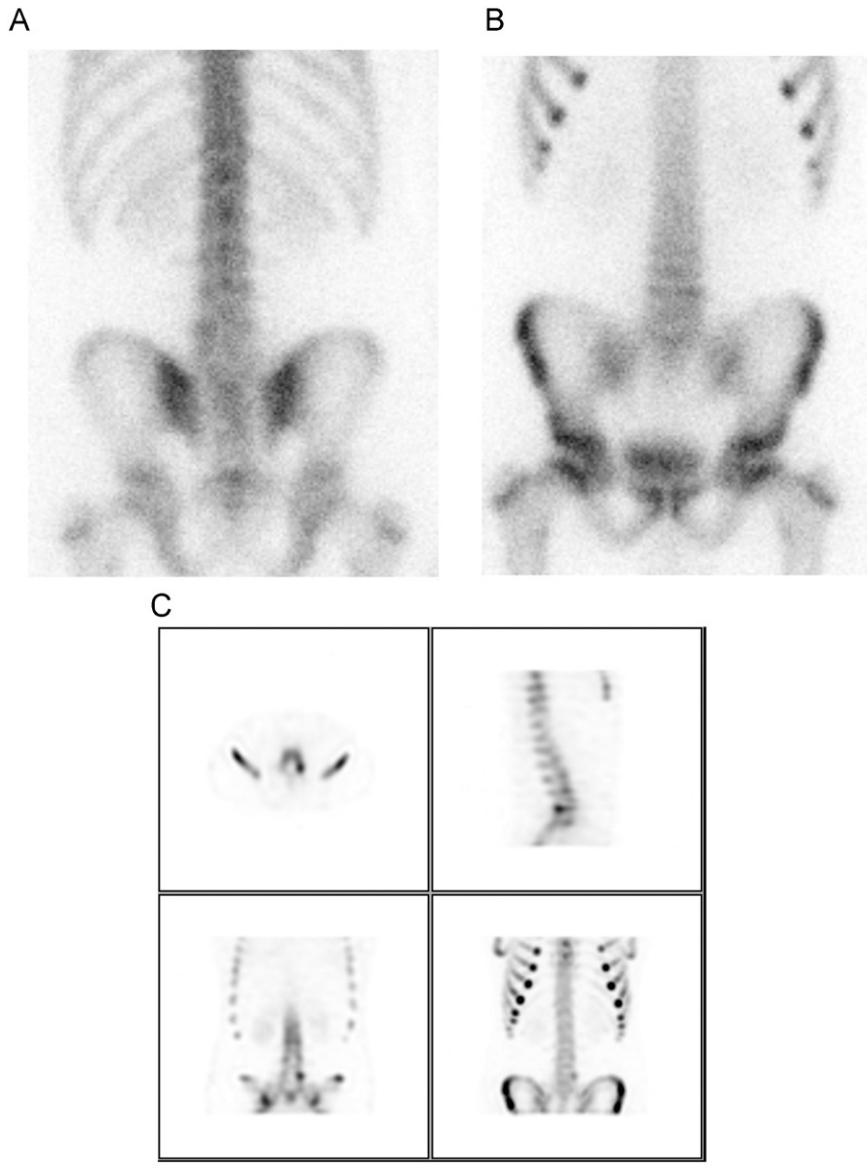

Figure 8 Bone scan in a 14-year old boy with chronic low back pain. Planar bone scan (A) posterior and (B) anterior did not show any significant focal increased uptake. (C) SPECT images (axial, sagital, coronal, and 3 dimensional views) show a focal increased uptake in the left L4-5 facet typical for spondylolysis.

Spondylolysis represents a stress fracture of the pars interarticularis of the vertebrae that occurs most commonly in the lower lumbar spine secondary to repetitive minor trauma such as hyperextension. However, congenital weakness of the pars as a result of hereditary factors also plays a role in its pathogenesis. Most patients present with either acute or chronic back pain. The sports most commonly associated with spondylolysis are gymnastics, diving, ballet, and contact sports such as football, hockey, and lacrosse. Bilateral spondylolysis may cause spondylolisthesis. Pars defects can be imaged with plain radiography, bone scintigraphy, CT, and MRI. In bone scintigraphy, spondylolysis produces little or no abnormality on blood pool images. Delayed images typically show focally high uptake in the region of the pars interarticularis. SPECT imaging is more sensitive than planar studies and will detect abnormalities in about one third of individuals with normal planar exams and is recommended in evaluation of low back pain in young athletes (Fig. 8)[68].

Low back pain may arise from stress associated with a lumbosacral transitional vertebral articulation which is a common congenital anomaly characterized by an enlarged transverse process and a non-ossified articulation with the sacrum.[69,70] Skeletal scintigraphy can show focally increased uptake along the transverse-sacral articulation of the transitional vertebra which supports the diagnosis of stress associated injury with a lumbosacral transitional vertebrae. As for spondylolysis, a SPECT study is superior to planar images and is recommended.[55,71]

In child abuse, bone scintigraphy is a complementary imaging modality to skeletal survey in diagnosis and management. Both modalities can be performed when child abuse is suspected.[72] Bone scintigraphy is useful when radiographs

are normal or detection of additional fractures would help in confirming the diagnosis. It can provide a quick assessment to characterize the extent and severity of trauma. Bone scintigraphy is more sensitive than radiographs for detection of rib fractures and nondisplaced diaphyses fractures of the extremities but less sensitive for skull or symmetrical metaphyseal fractures. Typically, rib fractures occur laterally, anteriorly, and posteriorly near the costovertebral junction where the ribs are compressed against the transverse process.[73] ^{18}F-NaF PET has been evaluated for assessment of pediatric patients with suspected abuse. Drubach et al. obtained PET images in 22 children younger than 2 years. A total of 156 fractures were detected at baseline skeletal survey, and 200 fractures were detected by PET with a sensitivity of 85% for the detection of all fractures and 92% for the detection of thoracic fractures including ribs, sternum, clavicle, and scapula. However, the sensitivity was relatively lower for the detection of metaphyseal lesions compared to the skeletal survey. The authors concluded that ^{18}F-NaF PET has overall better sensitivity and was superior in the detection of rib fractures.[74]

Fever of Unknown Origin (FUO)

FUO is defined in pediatric populations as a fever >38.3 °C of at least 7-10 days duration, without an apparent diagnosis after initial outpatient or hospital evaluation that includes a careful history and physical examination and inpatient assessment. The term fever without a source is used when the fever lasts for 7 days or less after a thorough clinical history and physical examination. Overall, in pediatric population, infections demonstrate as the predominant etiology for FUO in multiple studies.[75] In several studies, despite using modern laboratory tests, the cause of FUO remained uncertain in some children and the diagnosis was not established.[76,77]

After repeated careful history and physical examination and initial laboratory tests, further evaluation with specific laboratory examinations and diagnostic imaging as the second line investigations is warranted. Generally, the order and pace of these examinations are guided by the severity of illness and the result of initial studies.

Three-phase bone scintigraphy is both sensitive and specific for the diagnosis of osteomyelitis in non-violated bone and is often performed in the evaluation of children with FUO. Whole body bone scan is useful for localization of bone lesions, especially in younger children or those who cannot communicate or localize their pain (autism, cerebral palsy, etc.). Bone scan is not specific for differentiation of infection and inflammatory process vs tumors. However, this is not a disadvantage in the setting of FUO since the localization of the underlying pathology is of interest and further evaluation will clarify the exact pathology. It is important to pay attention to subtle soft tissue uptake which may identify non-osseous lesion.

Although, there are some controversies about using ^{67}Ga in patients with FUO, ^{67}Ga scintigraphy was considered the first-line nuclear medicine method for investigation of FUO in adult patients.[78] ^{67}Ga scan shows acute, chronic, granulomatous infections, noninfectious inflammatory foci and some malignant tumors. ^{67}Ga scanning has little role in pediatrics for detection of the underlying disease if the patients have systemic symptoms, but it may be useful in the cases of localized symptoms.[79] However, the relatively high radiation dose and the need to wait for several days until the study is completed make it an undesirable procedure. The usual administered activity in children is 1.5-2.6 MBq/kg (0.04-0.07 mCi/kg) with a minimum dose of 9-18 MBq (0.25-0.5 mCi). Detection of abdominal pathology is sometimes difficult due to physiological bowel activity in ^{67}Ga scan. Bowel activity is a common cause for both false-positive and false-negative results in ^{67}Ga study. SPECT scan and delayed images are essential in most cases.

^{99m} Tc or ^{111}In-white blood cell (WBC) scan is a useful imaging technique for visualization of infection (including intra-abdominal abscess, osteomyelitis, and infected prosthesis) and inflammatory bowel disease. The sensitivity and specificity of labeled WBC is relatively high for the detection or for ruling out infection; however, it is usually negative in other causes of FUO, particularly in tumors. The reported sensitivity and specificity of labeled WBC for the detection of infection as the cause of FUO was variable with a sensitivity of 55%-85% and specificity of 74%-94% for adults.[80] In children, the information is very limited and it is probably useful in selected cases.

Several studies have been reported regarding the use of ^{18}F-FDG-PET or PET/CT in patients with FUO over the past 2 decades. ^{18}F-FDG was helpful in 16%- 89% of patients with FUO.[81] In children, Jasper et al. retrospectively evaluated 69 children with FUO.[8] ^{18}F-FDG-PET or PET/CT scans were helpful in the diagnosis of 45% of the cases which was equivalent to those which were reported in adults. The final diagnosis was established in 54% of those patients, and among them, ^{18}F-FDG studies were contributory in 73%. The age of the patients did not seem to have a great influence on the result and the usefulness of ^{18}F-FDG scan. Moreover, laboratory, demographic or clinical parameters of the children did not predict the usefulness of FDG-PET scan.[82]

Similar to ^{67}Ga scan, the high sensitivity and relatively low specificity of FDG-PET for the diagnosis of pathologic processes is considered as advantageous due to the wide spectrum of etiologies in FUO.[83] Because the most common 3 broad causes of FUO (infections, inflammatory/collagen vascular/vasculitis, and malignancy) can be detected by FDG-PET/CT, it is a valuable modality for localization of the possible pathology in FUO.[81,84] ADDIN EN.CITE ADDIN EN.CITE.DATA In other words, a negative ^{18}F-FDG study excludes most of the underlying pathologies. The sensitivity of FDG-PET/CT to detect the underlying pathology was shown to be higher in comparison to ^{67}Ga scintigraphy.[85] Recently, Yang et al. reviewed ^{18}F-FDG-PET in 54 children with FUO. PET was positive in 28 patients and negative in 26 cases. Sixteen out of 28 positive cases were confirmed to be true positive. Overall, PET/CT was helpful in detecting the source of FUO in 29.6%.[86] In summary, nuclear medicine imaging techniques have an important role in assessing the

etiology of FUO after the first line examinations. Three-phase bone scan, ^{67}Ga imaging, and labeled WBCs have specific roles as second line investigations in selected cases based on clinical and physical examinations and laboratory assessments. ^{18}F-FDG-PET has the potential to replace other imaging modalities and can be considered in the evaluation of fever of unknown origin in pediatric patients. ^{18}F-FDG-PET allows diagnosis of a wider spectrum of diseases in comparison to the labeled WBCs and is probably more sensitive than ^{67}Ga scanning and has significantly less radiation exposure. Moreover, the study is completed in a shorter period of time and allows for further radionuclide studies, if necessary.

References

1. Gilday DL: Specific problems and musculoskeletal imaging in children. In: Sandler MP, Coleman RE, Patton JA, et al., (eds): Diagnostic Nuclear Medicine. Philadelphia, PA: Lippincot Williams & Wilkins; 2003
2. Treves ST, Baker A, Fahey FH, et al: Nuclear medicine in the first year of life. J Nucl Med 2011;52(6):905-925
3. Gelfand MJ, Parisi MT, Treves ST, Pediatric Nuclear Medicine Dose Reduction Workgroup. Pediatric radiopharmaceutical administered doses: 2010 North American consensus guidelines. J Nucl Med 2011;52(2):318-322
4. Lassmann M, Biassoni L, Monsieurs M, et al: The new EANM paediatric dosage card. Eur J Nucl Med Mol Imaging 2007;34(5):796-798
5. Nakagawa TA, Ashwal S, Mathur M, et al: Guidelines for the determination of brain death in infants and children: An update of the 1987 Task Force recommendations. Crit Care Med 2011;39(9):2139-2155
6. Banasiak KJ, Lister G: Brain death in children. Curr Opin Pediatr 2003;15(3):288-293
7. Friedman NC, Burt RW: Cerebral perfusion imaging. In: Henkin RE, Bova D, Dillehay GL, et al., (eds): Nuclear Medicine. Philadelphia, PA: Mosby-Elsevier; 2006
8. Donohoe KJ, Agrawal G, Frey KA, et al: SNM practice guideline for brain death scintigraphy 2.0. J Nucl Med Technol 2012;40(3):198-203
9. Treves ST, Chugani HT, Bourgeois BF: Part 1 Brain. In: Treves ST, (ed): Pediatric Nuclear Medicine/PET. New York, NY: Springer; 2007
10. Okuyaz C, Gücüyener K, Karabacak NI, et al: Tc-99m-HMPAO SPECT in the diagnosis of brain death in children. Pediatr Int 2004;46(6):711-714
11. Wieler H, Marohl K, Kaiser KP, et al: Tc-99m HMPAO cerebral scintigraphy. A reliable, noninvasive method for determination of brain death. Clin Nucl Med 1993;18:104-109
12. Spieth ME, Ansari AN, Kawada TK, et al: Direct comparison of Tc-99m DTPA and Tc-99m HMPAO for the evaluation of brain death. Clin Nucl Med 1994;19:867-872
13. Sinha P, Conrad GR: Scintigraphic confirmation of brain death. Semin Nucl Med 2012;42(1):27-32
14. Coker SB, Dillehay GL: Radionuclide cerebral imaging for confirmation of brain death in children: The significance of dural sinus activity. Pediatr Neurol 1986;2(1):43-46
15. Facco E, Zucchetta P, Munari M, et al: 99mTc-HMPAO SPECT in the diagnosis of brain death. Intensive Care Med 1998;24(9):911-917
16. Ashwal S, Schneider S: Brain death in the newborn. Pediatrics 1989;84(3):429-437
17. Patocka C, Nemeth J: Pulmonary embolism in pediatrics. J Emerg Med 2012;42(1):105-116
18. Andrew M, David M, Adams M, et al: Venous thromboembolic complications (VTE) in children: First analyses of the Canadian Registry of VTE. Blood 1994;83:1251-1257
19. Buck JR, Connors RH, Coon WW, et al: Pulmonary embolism in children. J Pediatr Surg 1981;16(3):385-391
20. Biss TT, Brandão LR, Kahr WH, et al: Clinical features and outcome of pulmonary embolism in children. Br J Haematol 2008;142(5):808-818
21. Brandão LR, Labarque V, Diab Y, et al: Pulmonary embolism in children. Semin Thromb Hemost 2011;37(7):772-785
22. Van Ommen CH, Peters M: Acute pulmonary embolism in childhood. Thromb Res 2006;118(1):13-25
23. Stein EG, Haramati LB, Chamarthy M, et al: Success of a safe and simple algorithm to reduce use of CT pulmonary angiography in the emergency department. AJR Am J Roentgenol 2010;194:392-397
24. Ciofetta G, Piepsz A, Roca I, et al: Guidelines for lung scintigraphy in children. Eur J Nucl Med Mol Imaging 2007;34(9):1518-1526
25. Parker JA, Coleman RE, Grady E, et al: SNM practice guideline for lung scintigraphy 4.0. J Nucl Med Technol 2012;40(1):57-65
26. Gottschalk A, Stein PD, Sostman HD, et al: Very low probability interpretation of V/Q lung scans in combination with low probability objective clinical assessment reliably excludes pulmonary embolism: Data from PIOPED II. J Nucl Med 2007;48(9):1411-1415
27. Hagen PJ, Hartmann IJ, Hoekstra OS, et al: How to use a gestalt interpretation for ventilation-perfusion lung scintigraphy. J Nucl Med 2002;43(10):1317-1323
28. Webber MM, Gomes AS, Roe D, et al: Comparison of Biello, McNeil, and PIOPED criteria for the diagnosis of pulmonary emboli on lung scans. AJR Am J Roentgenol 1990;154(5):975-981
29. Hagen PJ, Hartmann IJ, Hoekstra OS, et al: Comparison of observer variability and accuracy of different criteria for lung scan interpretation. J Nucl Med 2003;44(5):739-744
30. Freeman LM, Stein EG, Sprayregen S, et al: The current and continuing important role of ventilation-perfusion scintigraphy in evaluating patients with suspected pulmonary embolism. Semin Nucl Med 2008;38(6):432-440
31. Stein PD, Gottschalk A, Henry JW, et al: Stratification of patients according to prior cardiopulmonary disease and probability assessment based on the number of mismatched segmental equivalent perfusion defects: Approaches to strengthen the diagnostic value of ventilation/perfusion lung scans in acute pulmonary embolism. Chest 1993;104:1461-1467
32. Glaser JE, Chamarthy M, Haramati LB, et al: Successful and safe implementation of a trinary interpretation and reporting strategy for V/Q lung scintigraphy. J Nucl Med 2011;52(10):1508-1512
33. Gelfand MJ, Gruppo RA, Nasser MP: Ventilation-perfusion scintigraphy in children and adolescents is associated with a low rate of indeterminate studies. Clin Nucl Med 2008;33(9):606-609
34. Kiratli PO, Aksoy T, Bozkurt MF, et al: Detection of ectopic gastric mucosa using 99mTc pertechnetate: Review of the literature. Ann Nucl Med 2009;23(2):97-105
35. Sfakianakis GN, Conway JJ: Detection of ectopic gastric mucosa in Meckel's diverticulum and in other aberrations by scintigraphy: ii. indications and methods—A10-year experience. J Nucl Med 1981;22(8):732-738
36. Warrington JC, Charron M: Pediatric gastrointestinal nuclear medicine. Semin Nucl Med 2007;37(4):269-285
37. Treves ST, Grand RJ: Gastrointestinal bleeding. In: Treves ST, (ed): Pediatric Nuclear Medicine/PET. New York, NY: Springer; 2007
38. McEvoy CF, Suchy FJ: Biliary tract disease in children. Pediatr Clin North Am 1996;43(1):75-98
39. Kiewiet JJ, Leeuwenburgh MM, Bipat S: A systematic review and meta-analysis of diagnostic performance of imaging in acute cholecystitis. Radiology 2012;264(3):708-720
40. Tulchinsky M, Ciak BW, Delbeke D: SNM practice guideline for hepatobiliary scintigraphy 4.0. J Nucl Med Technol 2010;38(4):210-218
41. Montini G, Tullus K, Hewitt I: Febrile urinary tract infections in children. N Engl J Med 2011;365(3):239-250
42. Faust WC, Diaz M, Pohl HG: Incidence of post-pyelonephritic renal scarring: A meta-analysis of the dimercapto-succinic acid literature. J Urol 2009;181(1):290-297
43. Björgvinsson E, Majd M, Eggli KD: Diagnosis of acute pyelonephritis in children: Comparison of sonography and 99mTc-DMSA scintigraphy. AJR Am J Roentgenol 1991;157(3):539-543
44. Temiz Y, Tarcan T, Onol FF, et al: The efficacy of Tc99m dimercapto-succinic acid (Tc-DMSA) scintigraphy and ultrasonography in detecting

renal scars in children with primary vesicoureteral reflux (VUR). Int Urol Nephrol 2006;38(1):149-152
45. Piepsz A, Ham HR: Pediatric applications of renal nuclear medicine. Semin Nucl Med 2006;36(1):16-35
46. Hardy RD, Austin JC: DMSA renal scans and the top-down approach to urinary tract infection. Pediatr Infect Dis J 2008;27(5):476-477
47. Mandell GA, Eggli DF, Gilday DL, et al: Procedure guideline for renal cortical scintigraphy in children. Society of Nuclear Medicine. J Nucl Med 1997;38(10):1644-1646
48. Mouratidis B, Ash JM, Gilday DL: Comparison of planar and SPECT 99Tcm-DMSA scintigraphy for the detection of renal cortical defects in children. Nucl Med Commun 1993;14(2):82-86
49. Applegate KE, Connolly LP, Davis RT, et al: A prospective comparison of high-resolution planar, pinhole, and triple-detector SPECT for the detection of renal cortical defects. Clin Nucl Med 1997;22(10):673-678
50. Brenner M, Bonta D, Eslamy H, et al: Comparison of 99mTc-DMSA dual-head SPECT versus high-resolution parallel-hole planar imaging for the detection of renal cortical defects. AJR Am J Roentgenol 2009;193(2):333-337
51. Rossleigh MA: The interrenicular septum. A normal anatomical variant seen on DMSA SPECT. Clin Nucl Med 1994;19(11):953-955
52. Treves ST, Harmon WE, Packard AB, et al: Kidneys. In: Treves ST, (ed): Pediatric Nuclear Medicine/PET. New York, NY: Springer; 2007
53. Connolly LP, Drubach SA, Connolly SA, et al: Bone. In: Treves ST, (ed): Pediatric Nuclear Medicine/PET. New York, NY: Springer; 2007
54. Ma JJ, Kang BK, Treves ST: Pediatric musculoskeletal nuclear medicine. Semin Musculoskelet Radiol 2007;11(4):322-334
55. Nadel HR: Pediatric bone scintigraphy update. Semin Nucl Med 2010;40(1):31-40
56. Bybel B, Brunken RC, DiFilippo FP, et al: SPECT/CT imaging: Clinical utility of an emerging technology. Radiographics 2008;28(4):1097-1113
57. Faden H, Grossi M: Acute osteomyelitis in children. Reassessment of etiologic agents and their clinical characteristics. Am J Dis Child 1991;145(1):65-69
58. Connolly LP, Treves ST: Assessing the limping child with skeletal scintigraphy. J Nucl Med 1998;39(6):1056-1061
59. Wegener WA, Alavi A: Diagnostic imaging of musculoskeletal infection. Roentgenography; gallium, indium-labeled white blood cell, gammaglobulin, bone scintigraphy; and MRI. Orthop Clin North Am 1991;22(3):401-418
60. Schauwecker DS: The scintigraphic diagnosis of osteomyelitis. AJR Am J Roentgenol 1992;158(1):9-18
61. Pennington WT, Mott MP, Thometz JG, et al: Photopenic bone scan osteomyelitis: A clinical perspective. J Pediatr Orthop 1999;19(6): 695-698
62. Tsao AK, Dias LS, Conway JJ, et al: The prognostic value and significance of serial bone scintigraphy in Legg-Calvé-Perthes disease. J Pediatr Orthop 1997;17(2):230-239
63. Conway JJ: A scintigraphic classification of Legg-Calvé-Perthes disease. Semin Nucl Med 1993;23(4):274-295
64. Comte F, De Rosa V, Zekri H, et al: Confirmation of the early prognostic value of bone scanning and pinhole imaging of the hip in Legg-Calvé-Perthes disease. J Nucl Med 2003;44(11):1761-1766
65. Skaggs DL, Kim SK, Greene NW, et al: Differentiation between bone infarction and acute osteomyelitis in children with sickle-cell disease with use of sequential radionuclide bone-marrow and bone scans. J Bone Joint Surg Am 2001;83-A(12):1810-1813
66. Drubach LA, Connolly LP, D'Hemecourt PA, et al: Assessment of the clinical significance of asymptomatic lower extremity uptake in young athletes. J Nucl Med 2001;42(2):209-212
67. Ishibashi Y, Okamura Y, Otsuka H, et al: Comparison of scintigraphy and magnetic resonance imaging for stress injuries of bone. Clin J Sport Med 2002;12(2):79-84
68. Sty JR, Wells RG, Conway JJ: Spine pain in children. Semin Nucl Med 1993;23(4):296-320
69. Connolly LP, d'Hemecourt PA, Connolly SA, et al: Skeletal scintigraphy of young patients with low-back pain and a lumbosacral transitional vertebra. J Nucl Med 2003;44(6):909-914
70. Bron JL, van Royen BJ, Wuisman PI: The clinical significance of lumbosacral transitional anomalies. Acta Orthop Belg 2007;73(6):687-695
71. Pekindil G, Sarikaya A, Pekindil Y, et al: Lumbosacral transitional vertebral articulation: Evaluation by planar and SPECT bone scintigraphy. Nucl Med Commun 2004;25(1):29-37
72. Mandelstam SA, Cook D, Fitzgerald M, et al: Complementary use of radiological skeletal survey and bone scintigraphy in detection of bony injuries in suspected child abuse. Arch Dis Child 2003;88(5):387-390
73. Conway JJ, Collins M, Tanz RR, et al: The role of bone scintigraphy in detecting child abuse. Semin Nucl Med 1993;23(4):321-333
74. Drubach LA, Johnston PR, Newton AW, et al: Skeletal trauma in child abuse: Detection with ^{18}F-NaF PET. Radiology 2010;255(1):173-181
75. Joshi N, Rajeshwari K, Dubey AP, et al: Clinical spectrum of fever of unknown origin among Indian children. Ann Trop Paediatr 2008;28(4):261-266
76. Pasic S, Minic A, Djuric P, et al: Fever of unknown origin in 185 paediatric patients: A single-centre experience. Acta Paediatr 2006;95(4):463-466
77. Steele RW, Jones SM, Lowe BA, et al: Usefulness of scanning procedures for diagnosis of fever of unknown origin in children. J Pediatr 1991;119(4):526-530
78. Bleeker-Rovers CP, van der Meer JW, Oyen WJ: Fever of unknown origin. Semin Nucl Med 2009;39(2):81-87
79. Buonomo C, Treves ST: Gallium scanning in children with fever of unknown origin. Pediatr Radiol 1993;23(4):307-310
80. Kjaer A, Lebech AM: Diagnostic value of (111)In-granulocyte scintigraphy in patients with fever of unknown origin. J Nucl Med 2002;43(2):140-144
81. Ergul N, Cermik TF: FDG-PET or PET/CT in fever of unknown origin: The diagnostic role of underlying primary disease. Int J Mol Imaging 2011. 2011: 318051 (abstract)
82. Jasper N, Dabritz J, Frosch M, et al: Diagnostic value of [(18)F]-FDG PET/CT in children with fever of unknown origin or unexplained signs of inflammation. Eur J Nucl Med Mol Imaging 2010;37(1):136-145
83. Oyen WJ, Mansi L: FDG-PET in infectious and inflammatory disease. Eur J Nucl Med Mol Imaging 2003;30(11):1568-1570
84. Love C, Tomas MB, Tronco GG, et al: FDG PET of infection and inflammation. Radiographics 2005;25(5):1357-1368
85. Meller J, Sahlmann CO, Scheel AK: 18F-FDG PET and PET/CT in fever of unknown origin. J Nucl Med 2007;48(1):35-45
86. Yang J, Chamroonrat W, Servaes S, et al: Efficacy of FDG PET/CT in the evaluation of fever of unknown origin in pediatric patients. J Nucl Med: 2012;53(suppl 1):2214. [abstract]